EXPERIMENTAL INVESTIGATION OF THE RELATIONSHIP BETWEEN IMPACT CRATER MORPHOLOGY AND IMPACTING PARTICLE VELOCITY AND DIRECTION

N.G. Mackay, S.F. Green, D.J. Gardner and J.A.M. McDonnell
Unit for Space Sciences
Physics Laboratory
University of Kent
Canterbury, Kent CT2 7NR
U.K.
Phone: 227 764000 ext. 3266, Fax: 227 762616

SUMMARY

Interpretation of the wealth of impact data available from the Long Duration Exposure Facility, in terms of the absolute and relative populations of space debris and natural micrometeoroids, requires three dimensional models of the distribution of impact directions, velocities and masses of such particles, as well as an understanding of the impact processes. Although the stabilised orbit of LDEF provides limited directional information, it is possible to determine more accurate impact directions from detailed crater morphology. The applicability of this technique has already been demonstrated (Mackay et al, 1993, ref 1; Newman et al , 1993, ref 2), but the relationship between crater shape and impactor direction and velocity has not been derived in detail.

We present the results of impact experiments and simulations:

1) impacts at micron dimensions using the Unit's 2MV Van de Graaff accelerator
2) impacts at mm dimensions using a Light Gas Gun
3) computer simulations using AUTODYN-3D

from which an empirical relationship between crater shape and impactor velocity, direction and particle properties we aim to derive. Such a relationship can be applied to any surface exposed to space debris or micrometeoroid particles for which a detailed pointing history is available.

INTRODUCTION

During analysis of LDEF surfaces, a large number of elliptical craters were observed. These have been interpreted as due to impacts from interplanetary dust or space debris at highly oblique angles (refs 1 and 2) although it has been suggested that they were caused by irregularly shaped impactors. If the former interpretation is valid then these impact sites provide an invaluable diagnostic tool for determination of impact directions and hence orbital distribution of space debris particles impacting LDEF surfaces.

A series of experiments and hydrocode simulations have been performed in order to investigate the relationship between impact parameters and crater morphology. If a relationship of this nature can be established, it will be possible to use this to help deconvolve the dust/debris environment.
Previous experiments which have been performed by other researchers have included

1) Oblique impacts into rock and rock dust
2) Oblique impacts into glass
3) Oblique impacts into lead
4) Oblique impacts into bumper shields

Most of the experiments into semi-infinite targets were investigating factors such as depth to diameter ratios or volume of the crater excavated, although the bumper shield studies did include hole shapes and angles. The majority of space exposed surfaces suitable for dust particle impact studies are effectively smooth metal semi-infinite or foil targets. We are therefore investigating the effects of impactors of known speed direction and composition onto such targets.

EXPERIMENTAL DETAILS

Accelerator

The first experiments were performed using a 2MV Van de Graaff accelerator (Green et al., ref 3). The accelerator contains a dust source of spherical iron (I1068) particles which are typically less than 10 µm in diameter. The dust is charged with an electric field and accelerated along an evacuated flight tube to velocities from 0.5 km s^{-1} to upwards of 25 km s^{-1} before impacting the target.

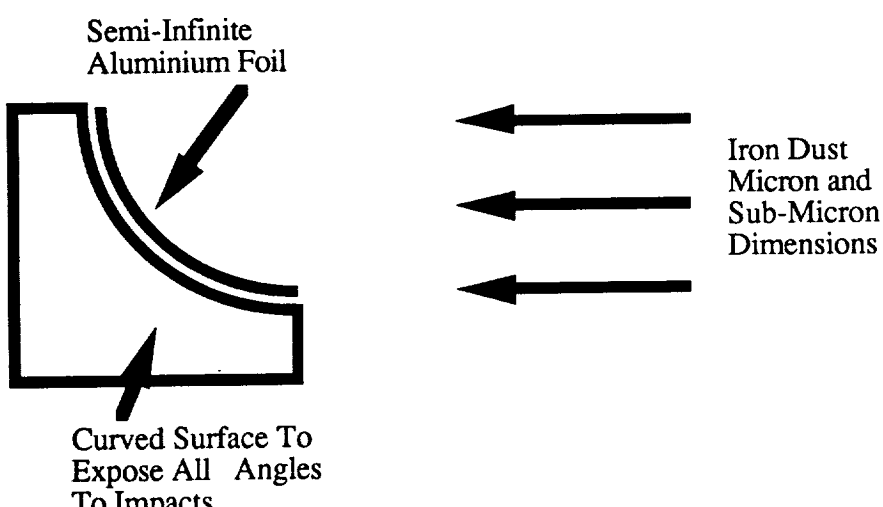

Figure1 Target frame and target used for the Van de Graaff accelerator experiment.

In this case the target was an aluminium foil curved round a target frame in order to expose the full range of angles of 0-90° to the impacting projectiles (as shown in figure 1).

After exposure in the accelerator the foil was removed from the mounting, flattened, and placed on a microscope stub. A preliminary analysis of it was performed using a Philips 525 SEM.

A strip down the length of the foil was examined, covering a range of angles from 90° to about 40°. Each crater located was classified according to its source (ie. hypervelocity or non-hypervelocity) and the quality of image achieved. Those craters from a non-hypervelocity source or with too poor an image to be useful were discarded and the remainder were then measured along both axes.

Light Gas Gun

The second phase of experimentation was performed using a two-stage Light Gas Gun.The Light Gas Gun can launch a solid nylon sabot (4mm in diameter) or smaller projectiles which are initially contained in a split nylon sabot that is stripped off in the flight chamber.

In this case steel ball bearings of 400 μm (AISI420C) and 1mm diameter were used as projectiles. These were fired at a series of discrete angled (55°, 65°, 70°, 75°, 85°) aluminium (HE30) targets (see figure 2). The accuracy of the target frame in defining the impact direction was measured and was found to be within 0.5° .

The targets were then removed from the target frame and the analysis was performed using an optical microscope.

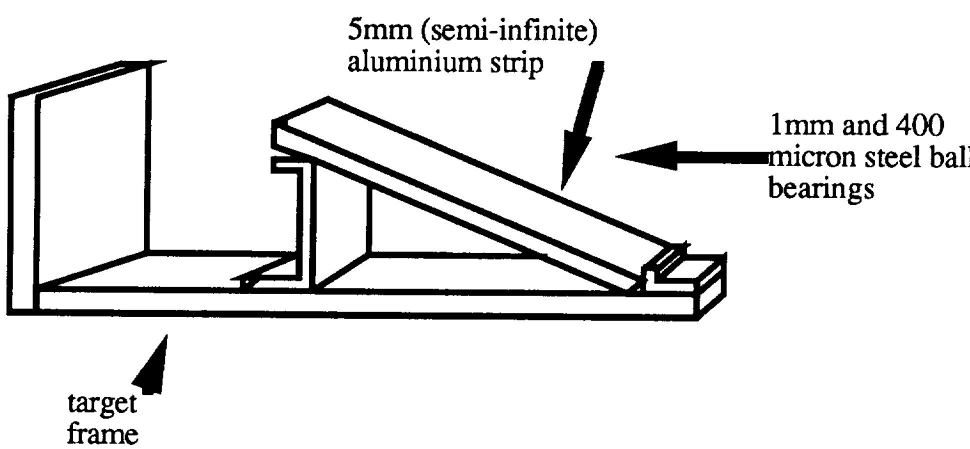

Figure 2: Target frame and target used for Light Gas Gun experiment.

AUTODYN-3D Simulations

AUTODYN-3D is an interactive, integrated hydrocode available on a very wide range of computers (ref 4). Currently a Lagrange processor exists in AUTODYN-3D, with other processors under development (the 2D version already incorporates Euler, ALE, and Shell processors as well).

Most hydrocodes (AUTODYN included) model materials as grids or arrays of cells, which either distort with the material (Lagrange method) or provide the calculation unit for material moving through the grid (Euler method). The Lagrange processor has the advantage of being computationally fast and gives good definition of material interfaces, but normally cannot simulate problems involving large deformations of the cells. This limitation can be overcome by the selective removal of cells, usually on the basis of a user-specified strain. The momentum and mass of these cells may be retained or discarded. Previous experience has shown that the best results (closest to experiment) are obtained by discarding the cells.

For the analyses reported here the Shock (Mie-Gruniesen) equation of state was used together with the Johnson-Cook strength model, thus continuing the data set of previous work (ref 5). All material data values used were exactly as published in references 6 and 7.

All the AUTODYN-3D simulations were Iron projectiles onto semi-infinite aluminium targets. The impacts so far simulated are 60°, 70° and 80° at 4 km s^{-1} and 80° at 16 km s^{-1}.

RESULTS

The preliminary results from the Van de Graaff accelerator experiment are shown in figure 3. Although the accelerator is capable of producing a large range of velocities these consist of small fast projectiles or larger slower ones. As a result of this it is difficult to analyse impacts from the very fast projectiles since they are very small and therefore produce craters which are too small to resolve with sufficient accuracy to determine ellipticity. In the case of the craters analysed so far the velocities were in the range 1-3 km s^{-1}. The craters are still noticeably elliptical at angles as small as 45° for these low velocities. The trend is very distinctly towards increased ellipticity with increased impact obliquity and in the range of 75-80° the craters become extremely long and thin.

Figure 4 shows examples of impact craters formed in the Light Gas Gun experiments with axis ratios plotted in figure 5. As in figure 3 the error bars are due to uncertainties in measurements. The scatter represents a real dispersion in crater properties. The velocities of the projectiles in the case of the Light Gas Gun were approximately (4.6±0.4) km s^{-1} which was slightly faster than the impacts so far measured from the accelerator experiments.

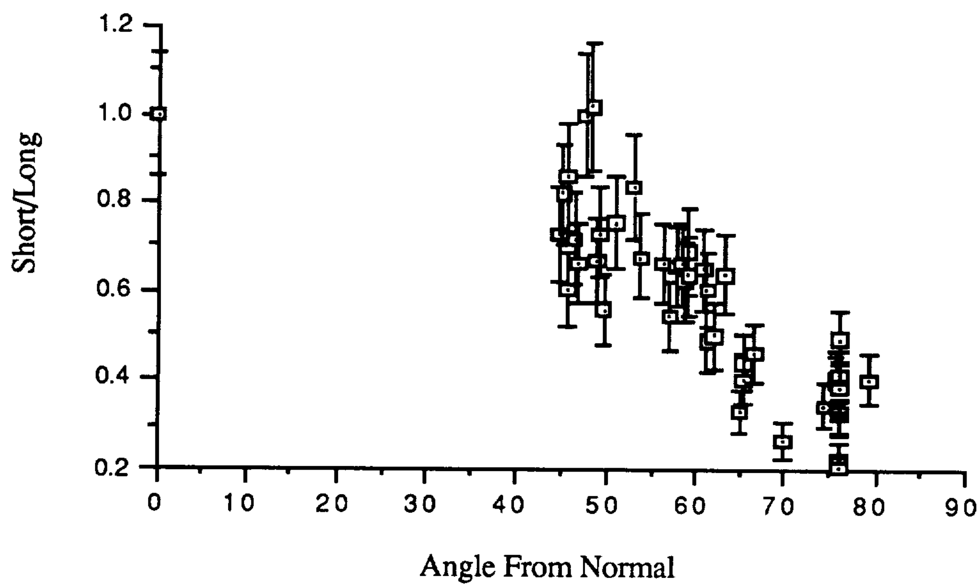

Figure 3: The variance of the ratio of short axis to long axis with angle of impact for craters produced by impacts from the Van de Graaff accelerator.

All impacts are from the left

55° 1mm ball bearing
Dimensions (mm) = (6.0±0.1) x (5.1±0.1)

65° 1mm ball bearing
Dimensions (mm) = (6.4±0.1) x (4.0±0.1)

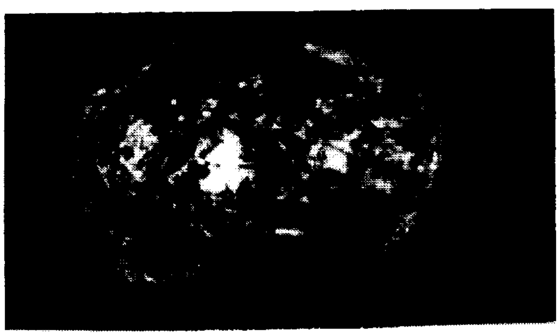

70° 1mm ball bearing
Dimensions (mm) = (5.9±0.1) x (4.6±0.1)

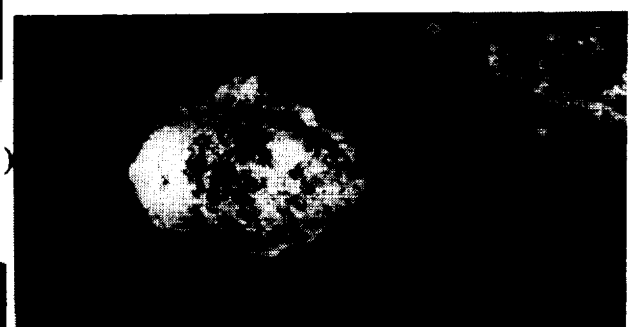

75° 1mm ball bearing
Dimensions (mm) = (5.2±0.1) x (3.1±0.1)
Notice the downstream ejecta

85° 1mm ball bearing
Dimensions (mm) = (5.9±0.1) x (1.0±0.1)
Note the multi-cratering

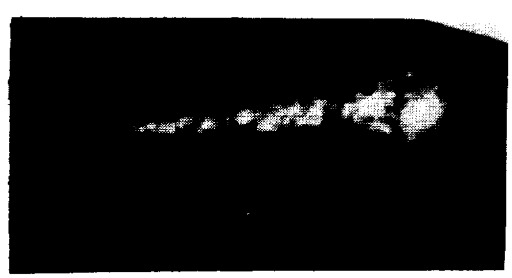

85° 400μm ball bearing
Dimensions (mm) = (1.7±0.1) x (0.9±0.1)
This example is unusual in that the craters increase in size along the line of flight instead of decreasing as normal.

Figure 4: Impact sites from light gas gun

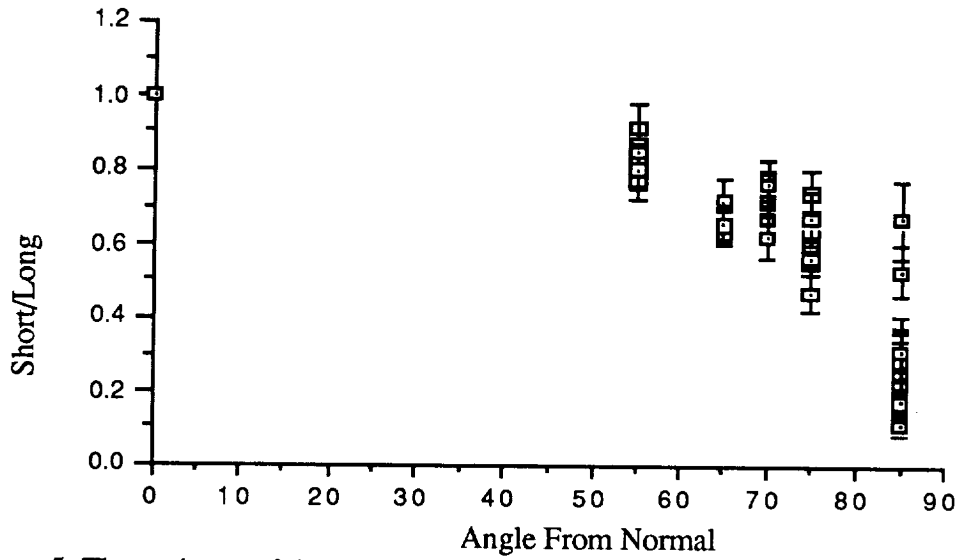

Figure 5: The variance of the ratio of short axis to long axis with angle of impact for craters produced by impacts from the Light Gas Gun.

The craters are noticeably less elliptical at lower angles than comparable impact sites from the accelerator, and as we reach very high angles (85°) multi-cratering begins to occur. (For the instances of multi-cratering the crater length is defined as the length of the longest single crater from the impact.)

Figure 6 shows data taken from Christiansen et al.(ref 8) and converted for comparison with the accelerator and Light Gas Gun experimental results. These data are also the results of Light Gas Gun experiments but this time at the higher velocity regime of 6.5-7 km s^{-1} with aluminium targets and projectiles.

No elliptical craters were observed until 72°, but from there the craters become rapidly more elliptical until multi-cratering is observed at 82°. (In this case the length for multi-cratering sites is defined as the total damage length from an impact.) This data still, in general, follows the observed trend of less elliptical craters for higher velocities.

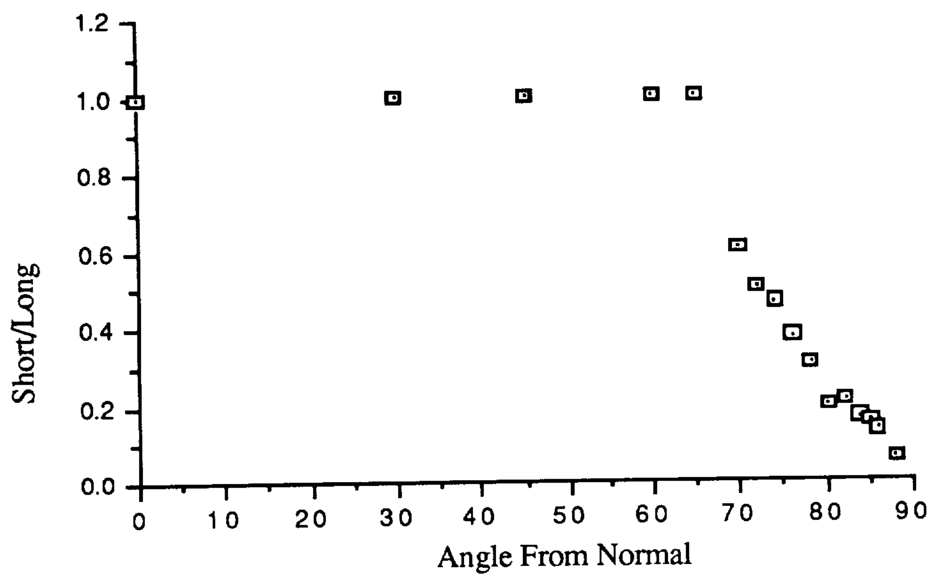

Figure 6: The variance of the ratio of short axis to long axis with angle of impact for craters produced by impacts from Christiansen et al (ref 8)

A comparison of all the data sets is shown in figure 7. The fits drawn to the data are by eye.

In general the data are consistent with the more oblique angles producing more elliptical craters, while increasing the velocity decreases the ellipticity for any given angle. Although Christiansen's data do cross the UKC Light Gas Gun data at about 75°, it is worth bearing in mind that his experiments were for aluminium impacts onto aluminium targets (as opposed to the iron onto aluminium of the UKC experiments) and his different definition of length used for multi-cratering sites.

The 4 km s^{-1} AUTODYN-3D simulations are consistent with the data but the 16 km s^{-1} AUTODYN-3D simulation shows a somewhat higher ellipticity than expected.

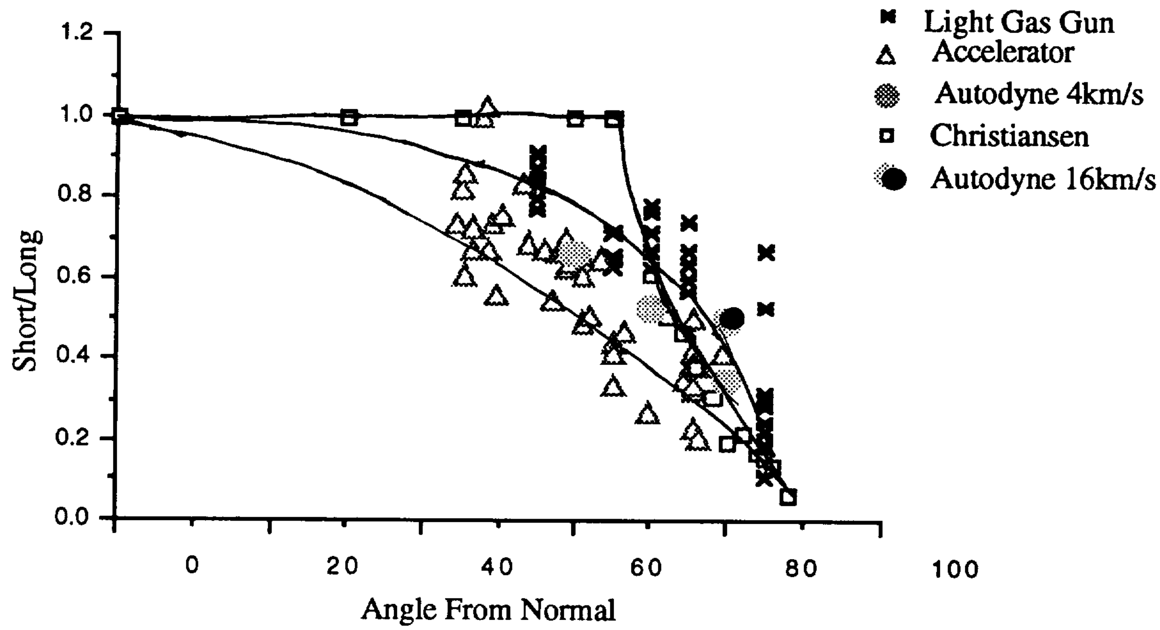

Figure 7: Comparison of results from figures 3, 5, 6

CONCLUSIONS

An experimental programme of hypervelocity impacts has demonstrated that it is potentially possible to use crater ellipticities to decode impact directions on space exposed materials. However we must take into account the differing impact velocities on each face of LDEF, and how this affects crater ellipticity, when attempting to decode impacts. Also we need an independent means of determining impact velocities, in order to deconvolve the effects of velocity and angle of impact. (It may be possible to use depth/diameter ratios of the crater for this.)

The relationship between the angle and velocity of the impact and the ellipticity of the crater requires further investigation and evaluation but we should also investigate the effect of parameters such as material properties, impactor size and shape, on the crater morphology.

The experimental program at UKC will continue with,

1) More curved surfaces being exposed in the Van de Graaff accelerator (future surfaces will be convex to avoid the danger of secondary impacts) using defined velocity windows and a variety of target materials (however only a restricted range of velocities can be investigated because of problems in analysing very small craters).

2)More angled targets in the Light Gas Gun with a variety of projectile sizes, target materials and projectile materials.

3) Establish that Hydrocodes agree with the experimental results at low (but still hyper) velocities and then use them to extrapolate to higher velocities where controlled experiments cannot be performed.

REFERENCES

1. Mackay, N.G., Green, S.F., Deshpande, S.P., and Newman, P.J., 1993. Interpretation of Impact Crater Morphology and Residues on LDEF using 3-D Space Debris and Micrometeoroid models. Proc. 1st European Conference on Space Debris, Darmstadt, 5-7 Apr. 1993.

2. Newman P.J., Mackay N., Deshpande S.P., Green S.F. and McDonnell J.A.M., 1993. Derivation of Particulate Directional Information from Analysis of Elliptical Impact Craters. Proc. Second LDEF Post-retrieval Conference, NASA CP-3194, 1993.

3. Green, S.F., Clarke, C. D. , and Stevenson, T. J., 1988. A 2MV Van de Graaff Accelerator for Cosmic Dust Simulation. JBIS Vol. 41 No. 9, Sept 1988.

4. Cowler, M., et al. AUTODYN - An Interactive Non-Linear Dynamic Analysis Program for Microcomputers through Supercomputers, 9th International Conference on Structural Mechanics in Reactor Technology, Lausanne, Aug.1987.

5. J.A.M.McDonnell, D.J.Gardner, P.J.Newman, N.J.Robertson, C.J.Hayhurst. Hydrocode Modelling In The Study Of Space Debris Impact Crater Morphology. Proc. 1st European Conference on Space Debris, Darmstadt, April 1993.

6. Group GMX-6, Selected Hugoniots, Los Alamos Scientific Lab. LA-4167-MS, May 1969.

7. Johnson and Cook, A Constitutive Model and Data for Metals Subjected to Large Strains, High Strain Rates and High Temperatures, Proc. 7th International Symposium on Ballistics, The Hague, 1983.

8. Christiansen, E.L., Cykowski, E., and Ortega, J., 1992. Highly Oblique Impacts Into Thick And Thin Targets. Journal of Impact Engineering, Nov. 1992.